Universidad Zaragoza
1542

Final Master Project

Development of Au Nanorods coated with mesoporous SiO_2 as SERS substrates for Gas Phase Detection

Author

Eduardo Bernad Quílez

Directors

Dra. María Pilar Pina Iritia

Dra. Reyes Mallada Viana

Master in Nanostructured Materials for Nanotechnological Applications

Department of Chemical Engineering and Environmental Technologies

Institute of Nanoscience of Aragon (INA)

Faculty of Science

2018-2019

Abstract

In this Final Master Project, core-shell Au-SiO_2 plasmonic nanostructures with adequate adsorption properties have been synthesized for their potential use as active material for detection of gas-phase neurotoxic agents by Raman-SERS (Surface Enhanced Raman Spectroscopy).

Firstly, the reproducible synthesis of gold nanorods with specific dimensions to ensure adequate optical properties in the VIS range was investigated. Secondly, the coating with a mesoporous silica shell of controlled thickness was carried out through chemical synthesis. Finally, different strategies for the removal of the template were attempted to identify the optimum that avoids reshaping of the gold core but ensure a high percentage of released pores, to improve the adsorption properties.

The morphological (size and shape), textural and optical properties of both, the gold nanorods and the prepared core-shell nanostructures have been characterized by transmission electron microscopy (TEM), UV-Vis absorption spectroscopy, dynamic light scattering (DLS) and N_2 physisorption.

Finally, they were deposited on glass substrates where their resonance plasmon was measured with the spectrophotometer.

INDEX

List of abbreviations

5-BrSA: 5-bromosalicylic acid

AR: Aspect Ratio

CTAB: Hexadecyltriethylammonium bromide

CTTS: Charge transfer to solvent

CW: Chemical Weapons

DTC: dithiocarbamate

EF: Enhancement Factor

FDTD: finite-difference time-domain

FMP: Final Master Project

MG: malachite green

NP: nanoparticle

NR: nanorod

SERS: Surface Enhancement Raman Spectroscopy

SPR: Surface Plasmon Resonance

TEM: Transmision Electron Microscopy

TEOS: Tetraethyl orthosilicate

TGA: thermogravimetric analysis

UV-Vis: Ultraviolet- Visible

VIS: Visible

1. Introduction

The research here in presented is within the framework of two main projects: AS^3: Advanced Sorption, SERS detection & Catalysis for CW threats (MICINN.CTQ20016-79419-R) and SENSOFT (Smart sensing for rapid response to chemical threats on soft targets (H2020-MSCA-RISE-2018/823895) which purpose, among others, the development of Raman-SERS (Surface Enhancement Raman Spectroscopy) based on technologies for selective and ultrasensitive detection of hazardous molecules in gas phase.

This Final Master Project comes up from my previous Final Machelor Degree Project in Chemistry [1], where a syntheis of core-shell Au-SiO_2 nanostructure was carried out. Unlike this FMP, gold nanoparticles (20 nm in size) were attached to a mesoporous silica core (120 nm in size), combining thus the required adsorption and plasmonic properties.

1.1 Raman-SERS spectroscopy and Materials

Spectroscopic techniques, such as Raman-SERS (*Surface Enhanced Raman Spectroscopy),* based on the use of radiation for the study of physical or chemical systems are gaining importance for portable chemical detection. Raman Spectroscopy is based on the phenomenon of the emitted photons, with lower energy and frequency than the incident one, of a system when a monochromatic light beam interacts with it (figure 1 a). Despite its high selectivity, information about the spectral fingerprint of the molecule, the sensitivity is quite low due to the inherent poor intensity of the inelastic scattering.

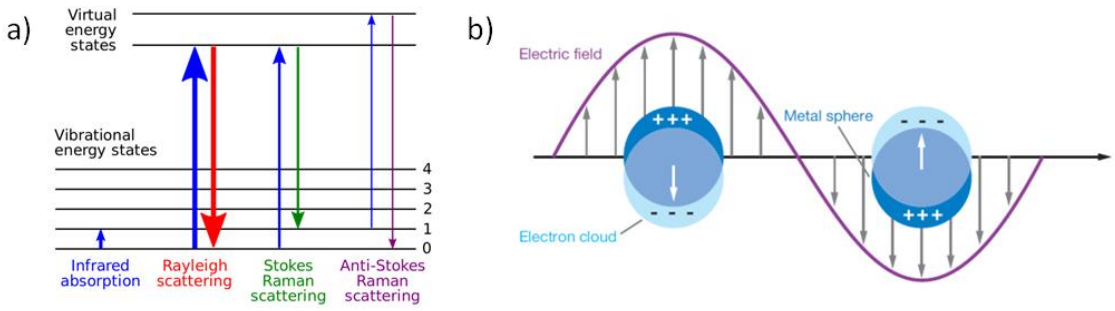

Figure 1. a) Energy level diagram showing the processes involved in the Raman spectroscopy. b) Schematic representation of the Surface Plasmon Resonance (SPR). Taken from [2]

Raman-SERS effect takes advantage of the so-called *Surface Plasmon Resonance* (SPR), the collective oscillation of the cloud of free electrons of the metallic nanostructure (figure 1 b), to amplify and enhance the intensity of the normal Raman signal of the targeted analyte. Nowadays, SERS is one of the leading techniques for label-free ultrasensitive vibrational fingerprinting of a variety of molecular compounds [3]. The molecular specificity of Raman signal together with the high sensitivity of the SERS technique has made it a highly demanded analytical tool.

The *Enhancement Factor* (EF) is the common parameter used to quantify the enhancement of the Raman signal obtained with respect to the Raman response under non-SERS conditions for the same molecule in the same environment of SERS effect. The SERS performance depends on several parameters including composition, size, morphology, topology, surface distribution, and dielectric environment of the metallic surface. Then, optimization of these parameters together with reliable and low cost methodologies for the preparation of homogeneous SERS substrates is a field of major interest.

In this work, metallic nanoparticles with localized SPR are pursued. According to the literature [4], the SPR occurs in metallic nanostructures made of silver and gold, between 10 and 200 nm in size, provoking an amplification of the electromagnetic field between 100 and 10,000 times greater in intensity than the incident field. In particular, this Final Master Project is focused on the use of gold nanostructures, discarding the use of silver cores due to its ease of oxidation. Besides, nanorods type morphology has been chosen due to the possibility to tune their aspect ratio, which results in different optical properties. A higher aspect ratio means having more elongated nanorods, and that the longitudinal surface plasmon band tends to nearer infrared wavelengths. Besides, an increase in the aspect ratio leads to an increase in the signal and the EF, and for the same aspect ratio, the signal will be higher the larger the rods. Therefore, this type of nanostructures has been used as sensors for various applications [5], such as food safety. For instance, gold nanorods are used for the SERS detection of pesticide residues in food, avoiding carrying out analyses that could contaminate food and provoke safety problem. These include the detection of malachite green (MG), a fungicide used against external parasites that can attack fish eggs in fish farms of Chine [6]. Another practical example of gold nanorods is the detection of Thiram (dithiocarbamate or DTC), a

fungicide used to protect fruit seeds against parasites. It can be applied during plant growth, or to prevent deterioration during storage or transport [7].

Previous to synthesis experiments, the plasmonic behaviour of gold nanorods was simulated in my working group by using finite-difference time-domain (FDTD) method by means of a commercial software package (Lumerical Solution Inc). The numerical results shows that gold nanorods with a width of 10 nm, a length of 40 nm, i.e. aspect ratio 2.66, provides with the higher electromagnetic field amplification (see Figure 2). In addition, this study confirms that this amplification is greater when the nanostructure is irradiated with a 633 nm laser line instead of 785 nm. Accordingly, this experimental work is mostly dedicated to achieve the synthesis of gold nanorods with such dimensions in a reproducible manner.

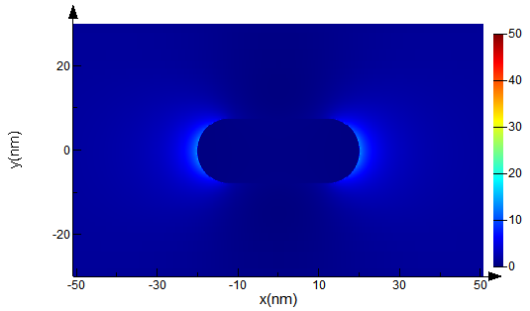

$L/W = 2.66. [E/E_0]^2_{max} = 11.8$

Figure 2. Schematic representation of the 2D simulation of the amplification of the electric field.

1.2 Au Nanorods based Nanostructures as SERS active materials

The ability to control the size and shape of metallic nanorods enables to tune their optical properties, i.e. SPRs. In fact, the optical properties of gold nanorods are especially important when their aspect ratio is larger than 1 [8]. According to the Gans' theory, due to the ellipsoidal shape of the nanorods, two different modes of absorption are observed, [9] the longitudinal and the transversal plasmonic bands (figure 3). The transverse mode, the weakest band, takes place when the electric field vector is perpendicular to the geometric axis, while the longitudinal bands take place when the electric field vector is parallel to the geometric axis [10]. The longitudinal plasmon band of absorption, in aqueous solution, is linearly proportional to the aspect ratio [9] [11] [12].

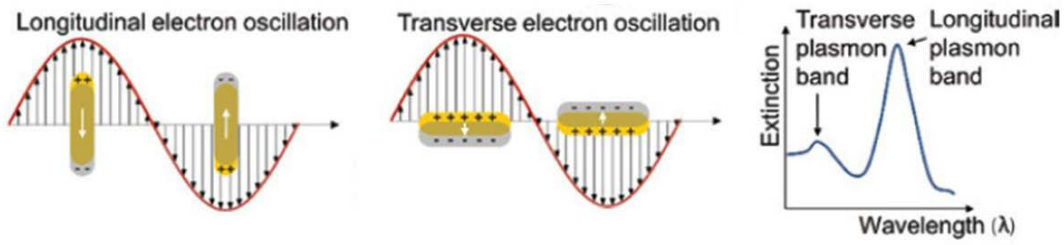

Figure 3. Schematically representation of the electron oscillation in the nanorods structures. Adapted from [13]

The seeds mediated growth method is the most widely reported in the literature to synthesize Au Nanorods. This method was first described by Jana et al. [14] in 2001. The $HAuCl_4$, chloroauric acid, precursor was reduced by ascorbic acid in the presence of a small number of silver ions and hexadecyltrimethylammonium bromide (CTAB) surfactant, that controlled and improved the nucleation and growth step. Herein, is worthy to note that the seeds' dispersion was prepared using sodium citrate instead of CTAB as capping agent. Subsequently, in 2002 El-Sayed et al. [8] introduced new improvements to the seed's synthesis, and replaced the presence of sodium citrate by CTAB in seed synthesis.

The synthesis of single crystalline gold nanorods by a wet chemical methodology could be described by the development of crystalline planes through surfactant surface-coated seeds (figure 4) as proposed by El-Sayed et al [8]. The growth takes place when the atoms of the seeds, protected by the positively charged headgropus of the CTAB, join to the (100) faces of gold nanocrystals lattice. As the growth and elongation of the structure occur, the formation of the new (100) faces ensures an effective protection of the growing structure by the surfactant micelles, clearly in escess. The transverse growth is less favoured than the longitudinal growth due to the best protection by the surfactant of the (100) faces.

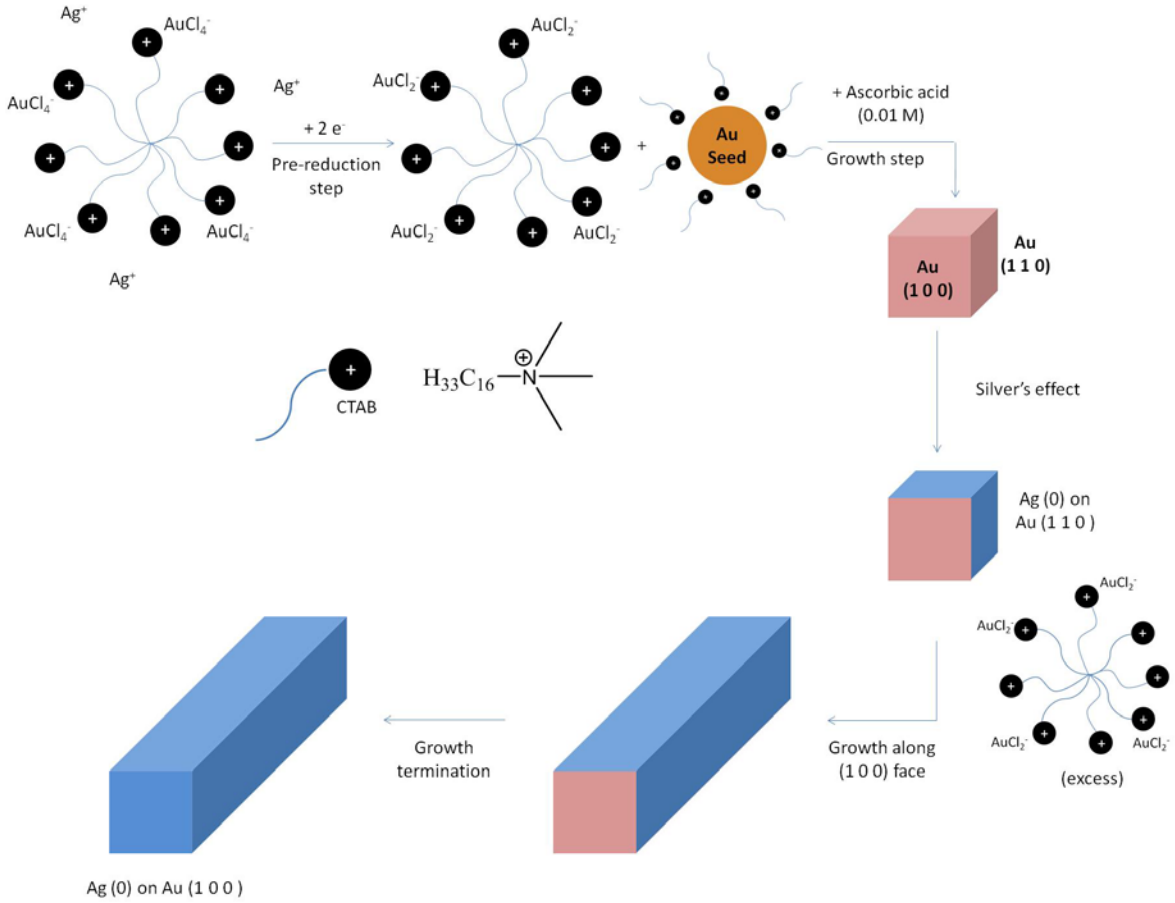

Figure 4. Schematic representation of gold nanorods growth's mechanisms. Adapted from [15]

The Au (III) of the [Au (III) − CTAB] micelles are reduced to Au (I), in the presence of 5-BrSA, as reducing agent. This step can be followed by the loss of absorbance at the 396 nm of the charge-transfer-to-solvent (CTTS) band. Later, during the growth step the collisions between [Au (I) − CTAB] and cationic gold seed particles take place. Then, there is a transport of the gold ions bound to the growing seed, controlled by the electric double layer interaction between the positively charged seeds and the negatively charged $AuCl_2^-$ on the surfactant micelles. The role of the silver ions is to interact with the anions of the CTAB, in order to reduce the charge density of these anions and improve the preferential interaction of gold and the surfactant on the exposed (100) faces.

The size and shape of metallic nanorods contributes significantly to the overall SERS signal, but the percentage of target molecules confined in such regions is also determining factor. In fact, the use of SERS substrate in the field of chemical sensing for gas phase detection is severely constrained by the adsorption of target molecules onto metallic nanostructures. Only molecules in the close vicinity of the enhancing

metallic surface (< 10 nm) can be detected. Thus why it is necessary to synthesize a nanostructure with plasmonic properties but also adequate sorption properties, i.e., large surface area.

The literature describes the synthesis of dense silica shells around metallic nanoparticles [16] [17], but there are few examples of the synthesis of a porous silica shell. Chen et al. [18] proposed the coating of gold nanorods with a shell of mesoporous silica for catalyst applications to improve the diffusion of the molecule and thus facilitate its contact with the metal core with catalytic activity. Sanz-Ortiz et al. [19] coated some gold nanorods with mesoporous silica, used as a template to grow the gold branches coming from the nucleus and thus better efficiency in the SERS assays was attained.

The synthesis of the shell is typically carried out by sol-gel process. The hydrolysis of a silica precursor in basic media in the presence of a surfactant acting as a template occur on the surface of the nanorods giving the pore structure. Synthesis time and the ratio SiO_2 precursor/pre-existing Au nanorods are the main parameters to determine the thickness of the shell.

The removal of the template, without affecting the gold nanostructure is the critical step of the preparation process. There are different options for removal such as: calcination, extraction and ozone treatment [19] [20] [21]. Calcination is usually the most classical methodology to remove the organic matter that constitutes the surfactant. In this work, liquid extraction and ozonation methods were proposed instead of calcination because the high temperature causes the reshaping of the metallic core, modifying its aspect ratio and, therefore, its plasmonic properties. In particular, template removal by liquid extraction under refluxing acid media [19] and ozonation [20] are mainly studied.

2. Objectives

The main goal of this work is to achieve a reproducible synthesis of gold nanorods (Au NR) as a plasmonic core, with an aspect ratio circa of 2.66, before coating them with a mesoporous silica shell of controlled thickness (below 50 nm) and release the mesopores in the least aggressive way, to preserve the metallic core and ensure a high percentage o free porosity (above 75%).

In order to achieve the objectives described in the previous section, the following tasks have been proposed:

- Synthesis of core-shell nanostructures, based on mesoporous SiO_2 and Au nanoparticles, that combine:
    - Adsorption properties of the mesoporous SiO_2 shell.
    - Plasmonic properties of the Au core.

- Physical-chemical and microscopy characterizations of these plasmonic nanostructures using UV-Vis absorption spectroscopy techniques, photon correlation spectroscopy, transmission electron microscopy (TEM).

- Incorporation of stable Au-SiO_2 Plasmonic Nanostructures on glass chips.

- Evaluation of the optical properties with the UV-Vis spectrophotometer.

3. Experimental

3. 1 Gold nanorods synthesis

The synthesis of gold nanorods is based on the work of Scarabelli et al [22]. We found that the control of the temperature is fundamental for synthesis reproducibility thus, all the steps, described below, were carried out in a controlled temperature bath at 28 ºC.

Pre-reduction step of the growth soltuion

For the pre-reduction step, 25 mL of CTAB (0.1 M) and 25 mg of 5-BrSA were placed in a 150 mL round bottom flask. Once it was dissolved, 480 µL of $AgNO_3$ solution (0.01 M) was added and stirred at 300 rpm for 15 min. Then, 25 mL of $HAuCl_4$ solution (0.001 M) was added in order to start the pre-reduction step.

The reduction of Au (III) to Au (I) was followed with UV-Vis (Agilent 8453 UV-Vis spectrophotometer). The absorbance measurements were carried out every 30 seconds in a 30 µL quartz cuvette with a path length of 1 cm, and the solution will be continuously renewed thanks to the use of an Agilent 1FS Peristaltic Pump. The peak selected to follow the reduction of gold it is at 396 nm corresponding to [Au (III) – CTAB] complex. Different pre-reduction times, ranging from 45 to 250 minutes, were studied.

Finally, the reaction was stopped at different selected times by the addition of 130 µL of ascorbic acid (0.1 M) under vigorous stirring.

Seeds formation step

In brief, in a 7 mL vial, set on a bath at 28 ºC, 4.7 mL of a CTAB (0.1 M) solution was mixed with 25 µL of a $HAuCl_4$ (0.05 M) solution. Once it was well dissolved, 300 µL of a cold $NaBH_4$ (0.01 M) solution was added under vigorous stirring for 2 minutes and then the solution was left undisturbed for 30 minutes, prior to use. In this step, it can be seen how after the addition of the reducing agent the solution loses its yellowish colour and becomes orange, what indicates the beginning of the nucleation of metallic gold and therefore the formation of the seeds. As the seeds' dispersion continues changing in colour, and consequently in size, over time, the evolution of the absorbance peak at 396 nm, corresponding to the [Au (III) – CTAB] micelles too, was

monitored along the 30 min reaction time to ensure reproducibility following the same procedure described in the pre-reduction step. A fresh seed solution was prepared for every synthesis of Au nanorods.

Nanorods growth

80 µL of the seeds dispersion was added on the growth solution, after controlled pre-reduction ensuring a correct mixing. Afterwards, the resulting solution was left undisturbed at 28 ºC. The evolution of the two plasmon resonance peaks of the nanorods was followed with a Jasco V-670 spectrophotometer. Finally, the dispersion was centrifuged 2 times for 25 min at 11000 rpm to remove all excess reagents and the surfactant. The pellet was resuspended in 5 mL of a CTAB (0.1 M) solution.

3.2 Synthesis of core-shell AuNR@mSiO$_2$

The protocol for the synthesis of a mesoporous SiO_2 shell around gold nanorods was carried out according to the literature [19] [23]. In addition, we tried to optimise the thickness of the silica shell by playing with the volumetric ratio of the gold nanorods and the silica precursor (see table 1). For this purpose, the amount of TEOS was kept constant while the amount of gold nanorods was modified.

Table 1. Variation of the volume ratio of reagents in the AuNR@mSiO$_2$ synthesis.

Experience	AuNR volume	$HAuCl_4$/TEOS	NP diameter
1	3.6 mL	47.84	~ 120 nm
2	5.0 mL	33.10	~ 100 nm
3	7.5 mL	22.07	~ 110 nm

In a 500 mL round flask, 75 mL of pure EtOH were mixed with 10.2 mL of a CTAB (0.1 M) solution and 159.8 mL of deionized water. Then, the solution was stirred for 30 minutes at 32 ºC before adding 100 µL of NH_3 (25 % wt) and the corresponding volume of gold nanorods dispersion (see table 1). After 5 minutes, 198 µL of TEOS (98 % wt) were added drop wise. After one minute stirring, the temperature was increased to 60 ºC, and once it was stabilized, the reaction was kept stirring for 2 days. The

resulting solution was centrifuged twice (12000 rpm for 20 minutes, 11000 rpm for 30 minutes) to eliminate the excess of reagents.

Surfactant removal

In this step, two different methodologies were studied in order to carry out a correct removal of the surfactant used as a template: calcination in an ozone environment [20] [24] and surfactant extraction under reflux in ethanol with hydrochloric acid. In the former approach, 10 mg of the compound is introduced in a cylindrical glass tube, leaving them supported on glass wool. The calcination was performed with a ramp of 5 ºC/ min to 200 ºC and holding it at this temperature for four hours, at the time an O_3 flux of 54 mL/min crosses the sample.

For liquid extraction, 10 milligrams of AuNR@mSiO_2 were introduced in a 250 mL three-neck round bottom flask with 80 mL of an HCl solution (0.1 M) in ethanol at room temperature. Then, the round bottom flask was immersed in an oil bath at 78 ºC at 300 rpm for 10 to 40 minutes, cooled down, and centrifuged twice for 20 minute at 10000 rpm. Finally, the pellet was collected and dried at 80 ºC overnight.

3.3 Plasmonic substrates

The incorporation of the sorbent and plasmonic material on Pyrex substrate of (5x8 mm^2) was carried out by drop coating. Firstly, a change of solvent, from water to ethanol, is carried out to improve the deposition process. The concentration of Au in different solutions are the following: 0.34 mg/mL of AuNR, 0.85 mg/mL solution of AuNR@mSiO_2 prepared by O_3 treatment, and 0.3 mg/mL of AuNR@mSiO_2 prepared by HCl (0.1 M) reflux.

The protocol of deposition consists on the addition of 25 µL. The addition of the AuNR@mSiO_2 treated with O_3 was repeated 6 times, while the AuNR@mSiO_2 treated with HCl (0.1M) was repeated 20 times and the AuNR naked addition was repeated 10 times. After that, the absorbance properties of the substrates in the UV-Vis region were measured with a Varian Cary 50 UV-Vis Spectrophotometer.

4. Results and discussion

4.1 Synthesis of AuNRs

Influence of the pre-reduction step in the final aspect ratio

The concept of pre-reduction step was introduced by Scarabelli et al [22]. These authors consider that the amount of Au (III) present into the solution, maintaining fixed the reaction conditions (temperature, amount reagents), before the addition of ascorbic acid (AA), notably influences the final aspect ratio of the gold nanorods.

During the pre-reduction step, Au (III) is reduced into Au (I) by the addition of the reductant 5-BrSA (5-Bromosalicylic acid) into the solution, decreasing the intensity of its yellow-orange colour. This change is monitorized in the UV spectrophotometer following the [Au (III) – CTAB] complex band at 396 nm, and is shown in the figure 5. This study helped us to determine the quantity of Au (III) reduced into Au (I) before the addition of ascorbic acid, and to compare our results with those published in the literature [22].

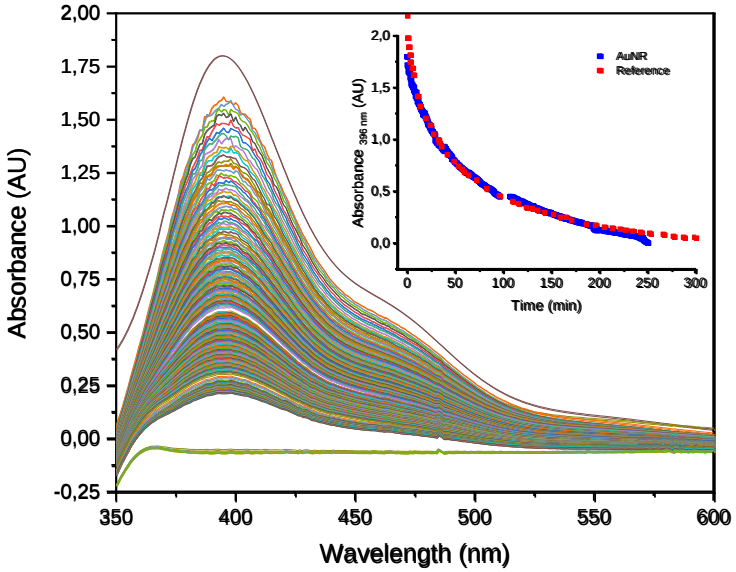

Figure 5. UV-Vis spectra corresponding to the pre-reduction step and insert of the variation of the absorbance with time at 396 nm, comparing with the reference [22].

Figure 5 shows the decrease in absorbance values of the reaction produced by the reduction of Au (III) by the 5-BrSA. In turn, in the inset of the figure, it can be seen that for a fixed reaction conditions (temperature, stirring, the amount of each reagent) the results agree with published literature [22].

Once the conditions for this pre-reduction step of the growth were established, TEM observation of the resulting NRs were carried out. Thermological study shows the new protocol is quite reproducible and that small-time variations in the pre-reduction time could lead to variations in the final aspect ratio of the nanostructures, and therefore in the longitudinal plasmon bands (850 to 550 nm) as can be observed in figure 6b. The study also indicates the presence of nanorods with aspect ratios close to one, for which lower ongitudinal/transversal band intensities (Figure 6a) are registered.

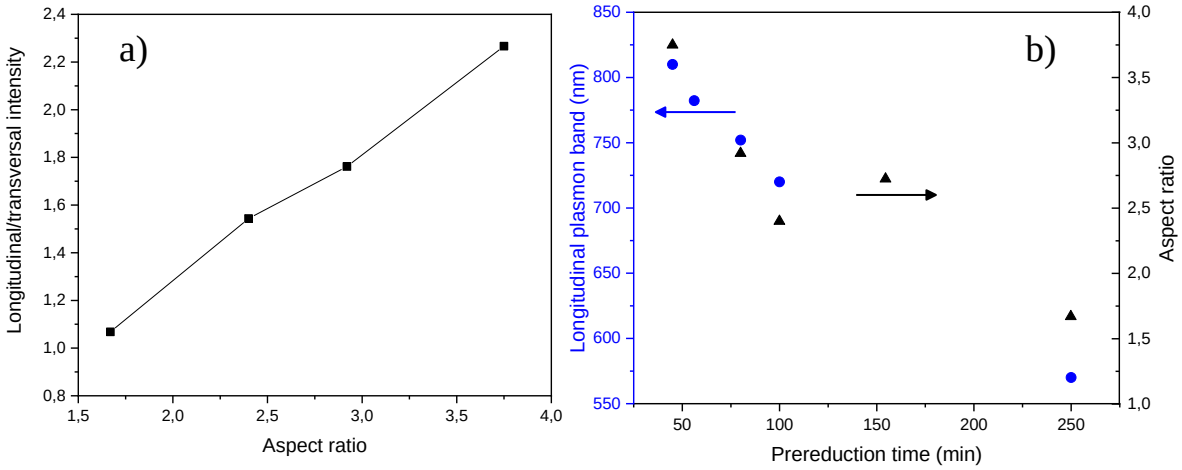

Figure 6. Relationship between a) the longitudinal/ transversal plasmon intensities according to the aspect ratio, b) the pre-reduction time and the final aspect ratio or the longitudinal plasmon band of the AuNR.

The influence of the pre-reduction time on the morphology and optical properties of the nanostructures is related to the amount of Au (III) species present in the reaction media, before being completely reduced to Au^0 by the addition of ascorbic acid, in agreement with the literature [22].

Seeds synthesis

As the seeds dispersion, used in this synthesis, varies in colour over time, a study of the evolution of the absorbance at 396 nm was also carried out (see Figure 7).

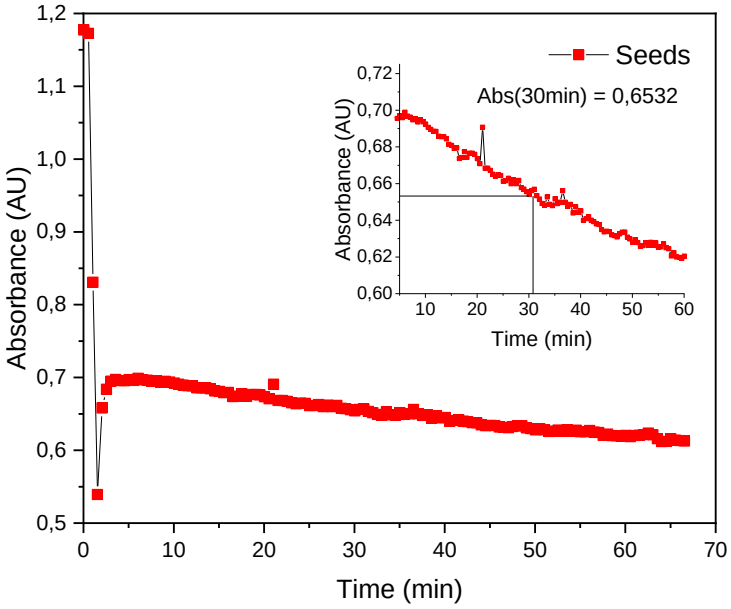

Figure 7. Variation of the seed solution absorbance at 396 nm with the time.

As we can see in figure 7, there is a quick reduction in the absorbance at short reaction time due to the addition of the $NaBH_4$, which corresponds to the reduction of Au (III), and after that, the solution slightly increases its colour due to the nucleation step. At this time the colour continuous decreasing, due to modification of seed's. For this reason, it was decided to fix a protocol to use always the same seeds' size. After the addition of the reductive agent with the gold solution, the stirring of the solution was kept constant for 2 seconds. After that, it was maintained undisturbed at 28 ºC for 30 minutes, to have the seeds formed with a specific size prior to their addition to the growth solution.

Growth synthesis

The growth step leads to the formation of the nanorods. For this step, we followed the reaction with the in the Jalisco UV-Vis equipment. After that, the gold

nanorods syntheses were characterized by UV-Vis spectrometer and by a Tecnai T20 Transmission Electron Microscopy (TEM). The *ImageJ analysis software* was used to estimate the aspect ratio of the gold nanorods from the TEM images.

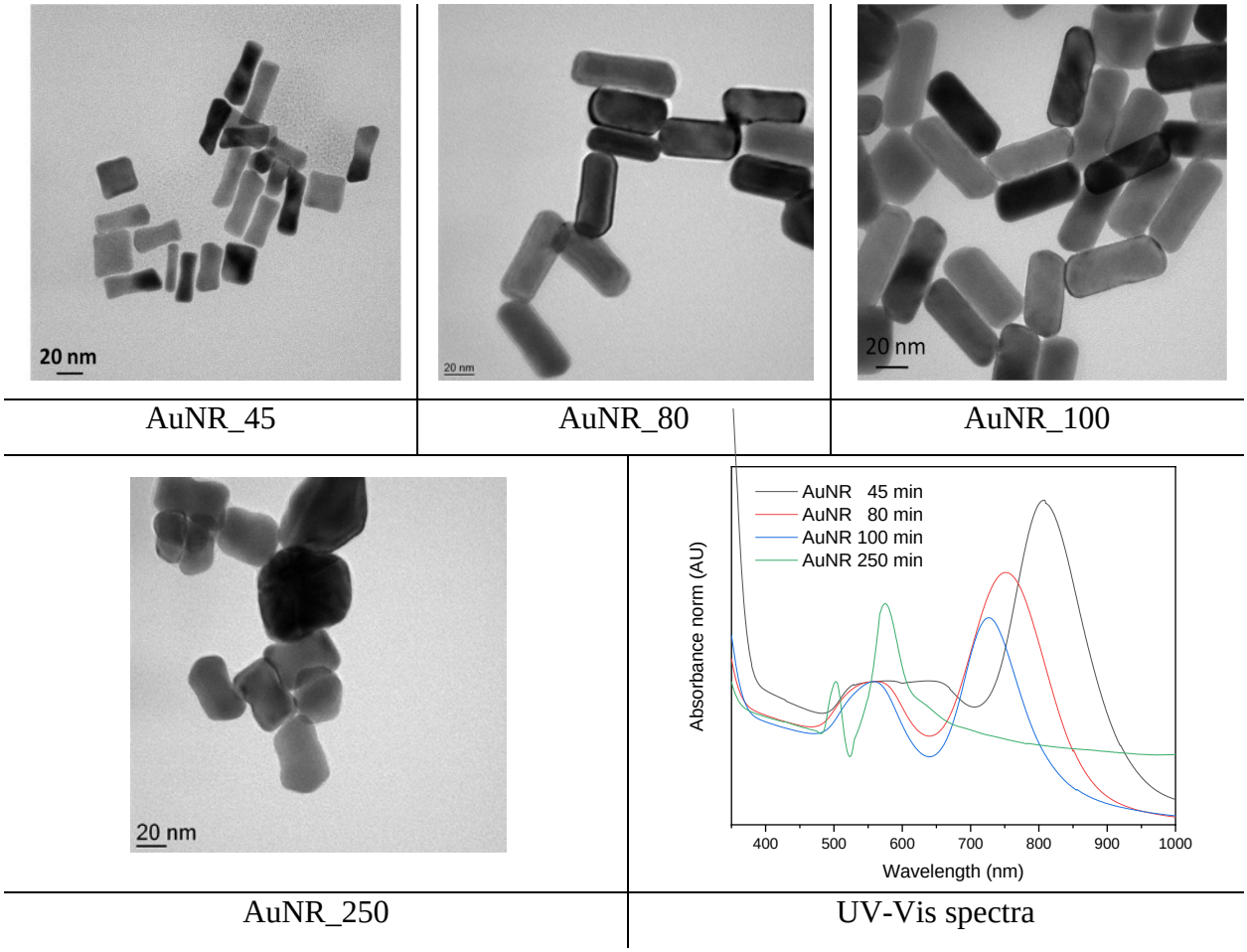

Figure 8. TEM images and UV-Vis spectra of AuNRs as function to the pre-reduction time

Figure 8 shows the TEM images and UV-Vis spectra of the different synthesized gold nanorods varying the pre-reduction time. The shorter the pre-reduction time, the more the longitudinal bands are displaced towards the NIR. In some cases, it is observed the dispersion in the morphology of the gold nanostructures, visible both in the TEM images and in the UV-Vis spectrum, a wideband appears around 530 nm typical of spherical nanoparticles. Literature indicates that with this method it is not possible to obtain a 100% selectivity to NRs since the formation of spheres or cubes [8] [14] [25] is thermodynamically preferred, despite the presence of surfactant and $AgNO_3$. Also, it can be observed that at the time the aspect ratio decrease, the ratio in the intensity of the plasmonic bands, and their distance in nm, also decreases.

Finally, the Z potential measurements of AuNRs show that at pH= 6.7 AuNRs have a positive surface charge (5.85 ± 0.35 mV).

4.2 Synthesis of core-shell AuNR@mSiO$_2$

Synthesis of mesoporous silica shell

This section covers the study carried out for synthesis of the mesoporous shell over the CTAB stabilized AuNRs with an aspect ratio of 2.6, i.e. 100 min as pre-reduction times. Firstly, variations in the volume of AuNR were carried out in order to study their influence on the final thickness of the silica shell (table 3).

Experience 3 shows an irregular result, despite the increase in the volume of nanorods, the total diameter of the nanoparticle also increases compared to experience 2. This result is attributed to the smaller size of the starting AuNR. Therefore, considering experience 1 and 2, and the TEM images shown in figure 9, the thickness of the silica shell increases with the TEOS/AuNR volumetric ratio.

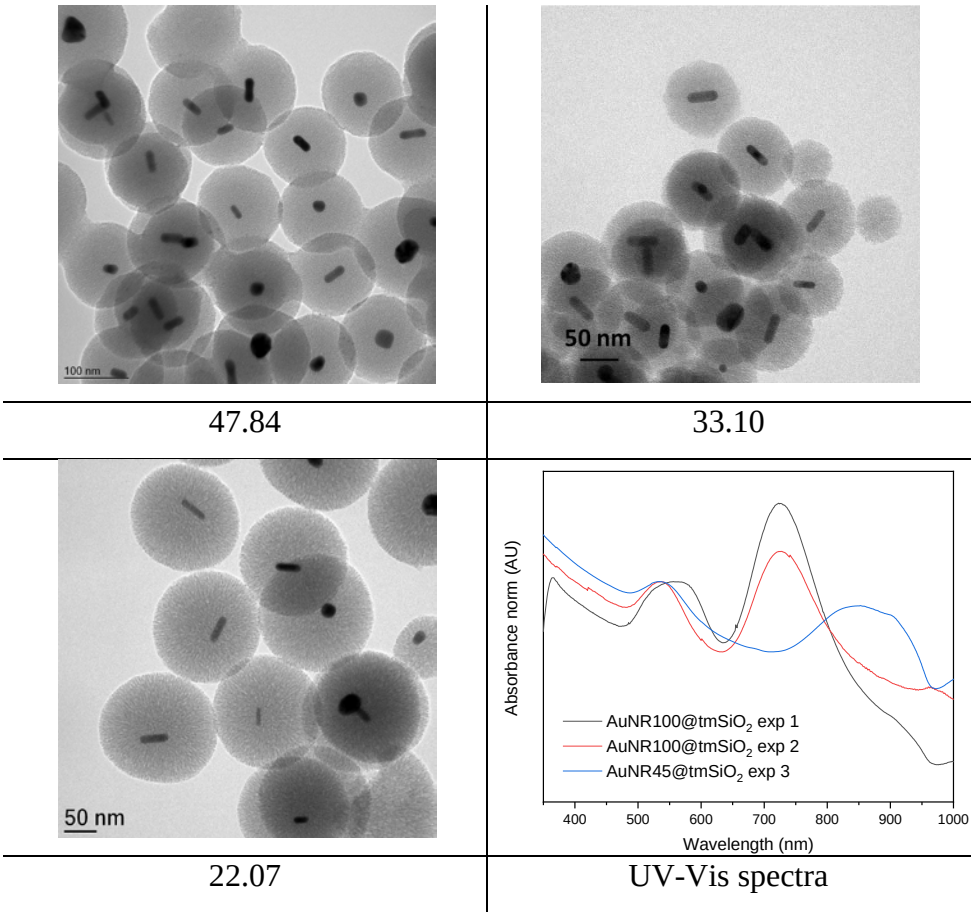

Figure 9. TEM images and UV-Vis spectra of AuNR@mSiO$_2$

Removal of the template from the mesoporous silica shell

The conventional method to remove the template of the mesoporous silica nanoparticles is by a calcination step at temperatures in the range of 450 to 500 ºC. Because of the presence of a metallic nanostructure as a core, we discard this methodology in order to avoid sintering. Instead we proposed calcinations with ozone and extraction (table 2) to have a preliminary evaluation of the efficiency, we firstly tested. The synthesis of MCM41 nanostructures was carried out according to the literature [21]. The synthesized MCM41 nanoparticles have a particle size of 400 nm.

Thermogravimetric analysis (TGA), up to 800 ºC in air atmosphere (50 mL/min) with a heating ramp o was used to quantify the percentage of template removal by comparasion with the control sample (no removal treatment applied). The sample before the removal step will show the weight loss (%) that correspond to the elimination of the surfactant present in the sample, in the temperature range between 200 and 300 ºC associated with the CTAB's decomposition. Once the data is obtained, the same TGA analysis is performed with the treated samples. An example of the calculations carried out has been detailed in the annexes for one sample (ANNEX I).

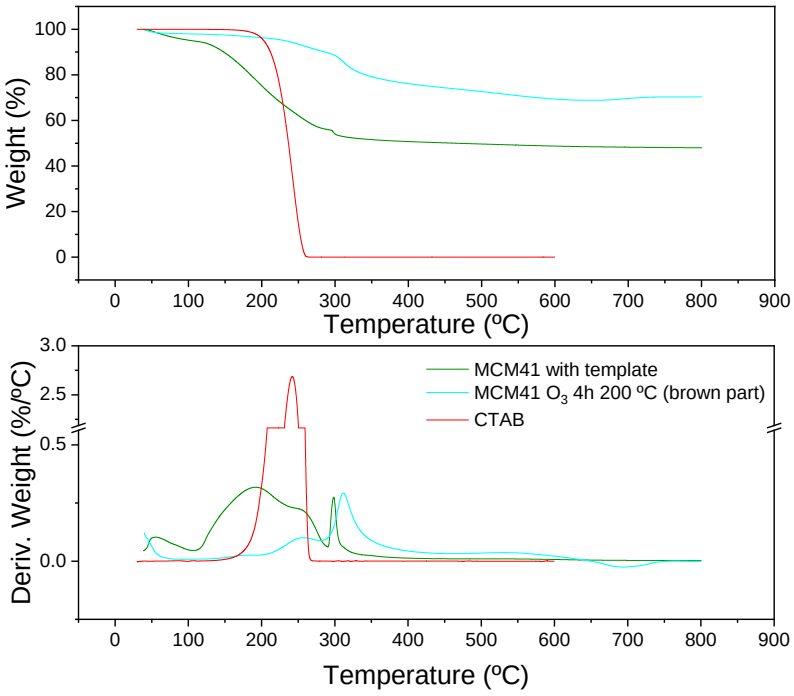

Figure 10. Representative graphs of TGA of MCM41 after a calcinations in O_3 environment.

Table 2. Experiments for template removal over MCM41 particles.

	Methodology		% wt template removed
1	Calcination	5 h at 500 ºC	100
		4 h O_3 at 200 ºC	61.1
2	Extraction	4 h EtOH	3.4
		1 h HCl (1.0 M) in EtOH	100
		1 h HCl (0.1 M) in EtOH	78.7
		2 h HCl (0.1 M) in EtOH	86.5

In the case of the extraction process, a complete removal of the surfactant was observed with a concentracion 1M of hydrochloric acid. When the concentration of HCl was decreased to 0,1M after 2h extraction the percentage of removal was 86,5%. The results of TGA were corroborated with the analysis of the nitrogen adsorption isotherm after the extraction process (figure 11 and Table 2) The total pore volume of the calcined or sample extracted with the highest concentration of acid was 0,89cm^3/g and this value was reduced to 0,77 and 0,70 when using 2h and 1h extraction with a concentration of 0,1 M of acid. Considering the high pore volume recovered and the softer conditions, we proposed to study mainly the use of HCl (0.1 M) ethanolic solution for AuNR@mSiO_2.

The first method consists on the calcinations of the silica mesoporous particle in an ozone environment. For this purpose, oxygen was introduced into the ozone generator (NEO500 of Neosyst company), with a flow of 52 mL/min, where the ozone is produced *in situ* thanks of an electric current of 16 mA. Then, ozone was introduced into a glass tube set inside a vertical oven. The calcination was performed with a ramp of 5 ºC/ min to 200 ºC and holding it at this temperature for four hours.

Table 3. Textual properties of MCM41 subjected to different template removal processes.

	Methodology		S_{BET} (m^2/g)	Pore volume (cm^3/g)	Pore size (nm)
1	Calcination	5 h at 500 ºC	1186.9 ± 25.8	0.89	2.5
		4 h O_3 at 200 ºC	-	-	-
2	Acid reflux	4 h EtOH	19.0 ± 0.1	0.03	3.3
		1 h HCl (1.0 M) in EtOH	1114.1 ± 20.3	0.89	3.2
		1 h HCl (0.1 M) in EtOH	1056.4 ± 4.2	0.70	2.6
		2 h HCl (0.1 M) in EtOH	960.9 ± 11.4	0.77	3.2

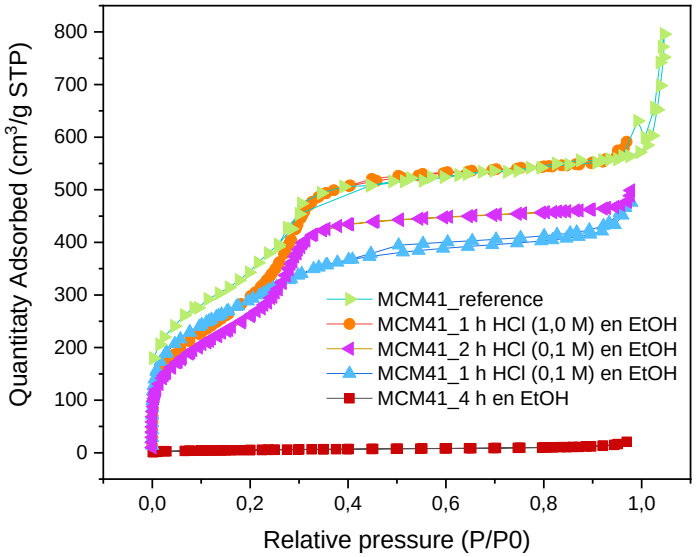

Figure 11. Representative curves of N_2 physisorption of MCM41 treated in different ways.

AuNR@mSiO$_2$

The experiments carried out for the template removal on AuNR@mSiO$_2$, are presented in the (table 4). Considering that the thickness of the shell was smaller, compared to the size of the MCM41 nanoparticles in the preliminary studies, the extraction time was varied from 10 to 40 minutes.

Table 4. Experiments carried out in the removal step for AuNR@$mSiO_2$.

	Methodology		% wt template removed
1	Calcination	4 h O_3 at 200 ºC	78.3
2	Acid reflux	10 min HCl (0.1 M) in EtOH	77.3
		20 min HCl (0.1 M) in EtOH	76.2
		30 min HCl (0.1 M) in EtOH	70.0
		40 min HCl (0.1 M) in EtOH	87.4

Ozone and AuNR@$mSiO_2$

When carrying out a softer cacination than those described in the literature [19], the TGA results show that the percentage of surfactant removed was close to 80 %, while TEM images (figure 12) shows that the gold nanostructures didn't lose their cylindrical shape after the calcinations. On the contrary, the UV-Vis spectrum shows that the intensity of the transversal band is higher than the longitudinal one due to the presence of a large population of nanoparticles. Our exploration relies on the $AgNO_3$ reagents, used in this batch (use of SS spatula for handling instead of plastic one)

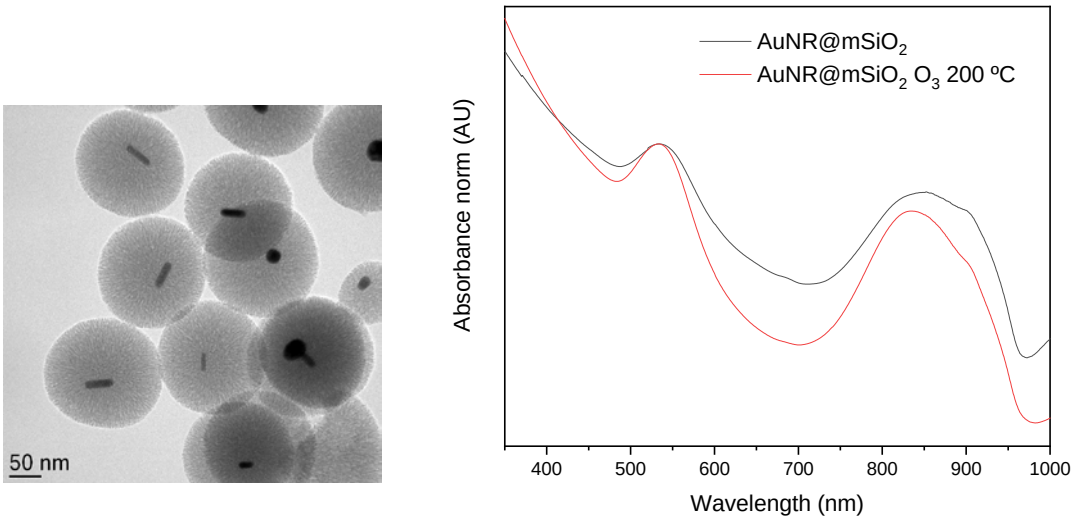

Figure 12. TEM images of AuNR@$mSiO_2$ before the treatment and UV-Vis spectra of AuNR@$mSiO_2$ before and after the O_3 treatment.

Ethanolic extraction under Reflux and AuNR@mSiO$_2$

Additionally, studies to know the influence of how acid reflux affects the gold core and the surfactant removal process were performed. Firstly, the previous study conditions (table 2), were adapted for a particle with a diameter 4 times smaller: 420 nm of MCM41 vs. 110 nm of AuNR@mSiO$_2$ (see table 4).

TEM images of figure 13 show that the external border of the silica shell seems to be damaged after 40 minutes of acid reflux. In addition, after the 40 minutes, gold nanorods shape seems almost unaltered in agreement with the registered UV-Vis spectrum. For this reason, the acid reflux is the chosen methodology to remove the template of the silica coating.

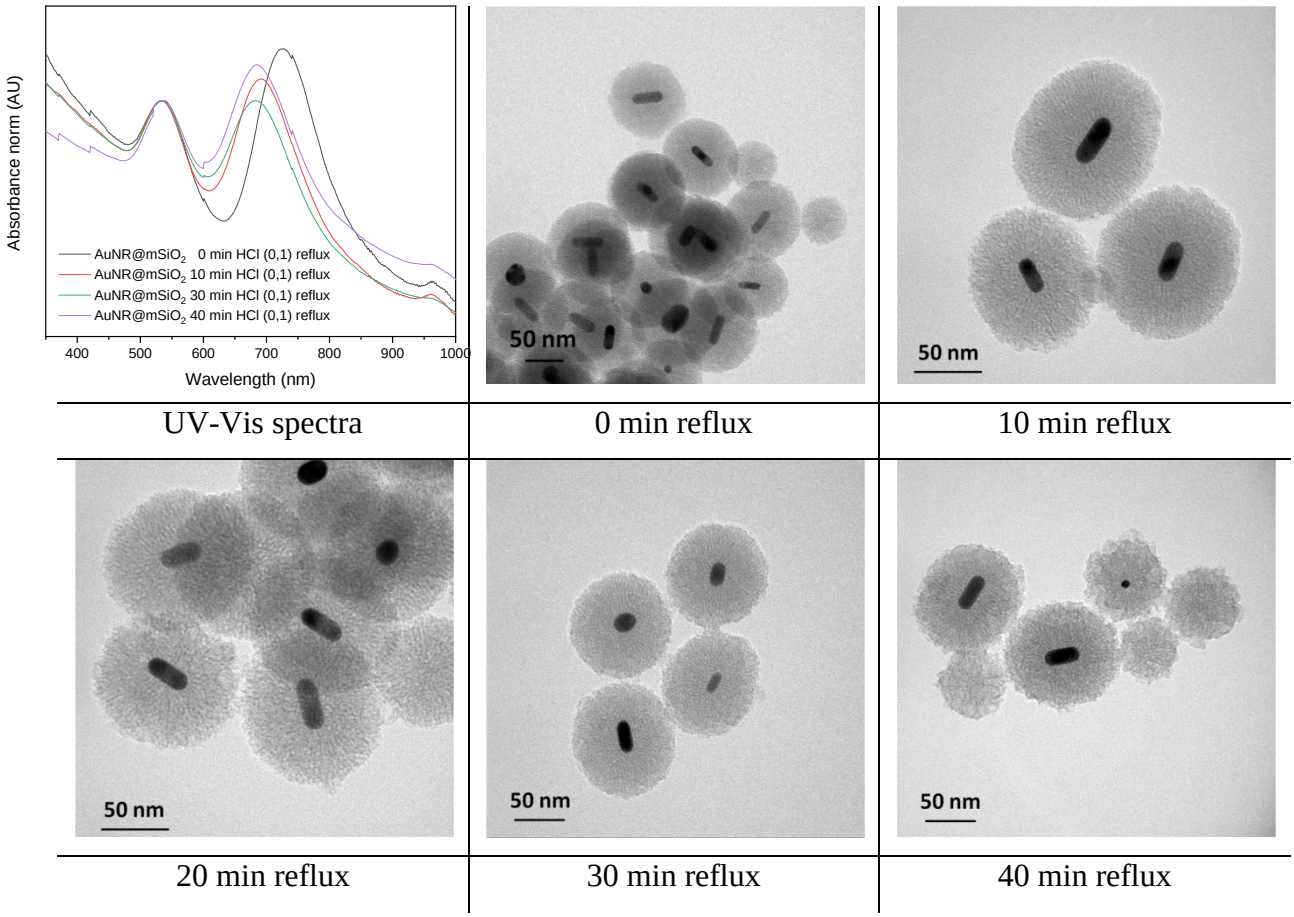

UV-Vis spectra	0 min reflux	10 min reflux
20 min reflux	30 min reflux	40 min reflux

Figure 13. TEM images and UV-Vis spectra of AuNR@mSiO$_2$ at different times of ethanolic reflux in HCl 0.1 M: a) 0 min, b) 10 min, c) 20 min, d) 30 min, e) 40 min.

It can be observed that at the extraction time increases, the longitudinal plasmon band is slightly shifted to the blue, while the transverse plasmon band remains fixed. It

could be explained because it may happen that in some cases the surfactant had been removed and the gold cores could be being affected by the acid solution.

Table 5. Results obtained with AuNR@$mSiO_2$ particles treated with different methods

Sample	% removed template	Thickness of shell with template (nm)
AuNR@$mSiO_2$ O_3	78.3	13.0
AuNR@$mSiO_2$ 10 min HCl 0.1M	77.3	13.7
AuNR@$mSiO_2$ 20 min HCl 0.1M	76.2	14.3
AuNR@$mSiO_2$ 30 min HCl 0.1M	70.0	18.0
AuNR@$mSiO_2$ 40 min HCl 0.1M	87.4	7.6

In the table 5 appears the final effective porous shell of AuNR@$mSiO_2$ and the % of removed template estimated by TGA for the different conditions. In order to carry out this analysis, we have to consider gold nanorod of 40 x 10 nm, a mesoporous silica shell of 3 nm of pore, and a final particle with a diameter of 120 nm. All calculations are shown in ANNEX II.

4.3 Substrate measurements

First of all, UV-Vis measurements of the different substrate prepared were carried out to know how the deposition of the nanostructures on substrates affects to their plasmonic properties.

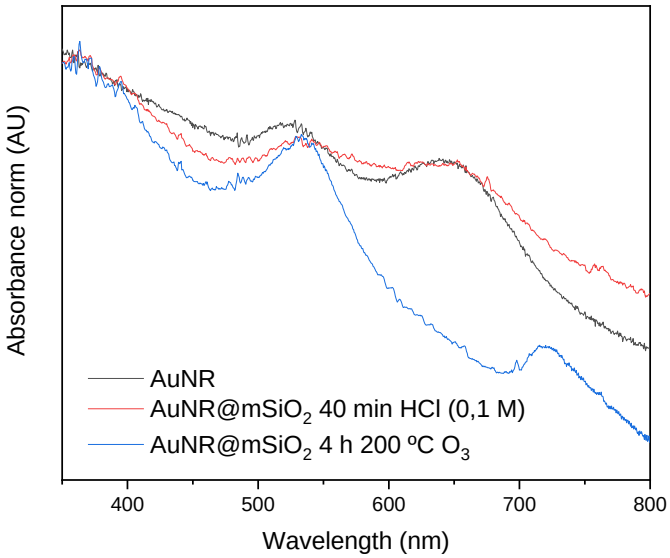

Figure 14. UV-Vis spectra of the plasmonic substrates

As it can be observed in the Figure 14, after carrying out the deposition the two characteristic bands that define the AuNRs resemble similar for both AuNRs and AuNR@mSiO2 reflux samples. On the contrary when compared with UV-Vis in solution, their relationship of intensities is reduced and the longitudinal band is shifted to smaller wavelength values.

5. Conclusions and future work

In this Final Master Project, a preparation procedure for metallic nanostructures with good adsorption properties and plasmonic properties has been stablished. First of all, a study of the gold nanorods synthesis have been carried out in order to obtain a nanostructure that provoke a high enhancement of the signal for the Raman-SERS measurements. Secondly, they were coated with a mesoporous silica shell thanks to the use of surfactant. Thirdly, different removal methods have been studied for the synthesis of gold nanorods coated with a real mesoporous shell, with the aim of not to damage the plasmonic properties of the metallic core. The acid reflux at 40 minutes shows a real alternative for the classical methods, due to controlling the time of this step we can achieve remove almost all the template. In addition, it means a fast and easy way to carry out this step.

Finally, as future work, a complete characterization of the steps of the synthesis has to be done, trying to reduce more the thickness of the silica shell. In addition, Raman-SERS measurements of the neurotoxic agent's simulant in gas phase have to be performed in order to check the real response of the SERS substrates.

References

[1] M. Lafuente *et al.*, «SERS Detection of Neurotoxic Agents in Gas Phase Using Microfluidic Chips Containing Gold-Mesoporous Silica as Plasmonic-Sorbent», en *2019 20th International Conference on Solid-State Sensors, Actuators and Microsystems & Eurosensors XXXIII (TRANSDUCERS & EUROSENSORS XXXIII)*, Berlin, Germany, 2019, pp. 1313-1316.

[2] K. A. Willets y R. P. Van Duyne, «Localized Surface Plasmon Resonance Spectroscopy and Sensing», *Annual Review of Physical Chemistry*, vol. 58, n.º 1, pp. 267-297, may 2007.

[3] B. Sharma, R. R. Frontiera, A.-I. Henry, E. Ringe, y R. P. Van Duyne, «SERS: Materials, applications, and the future», *Materials Today*, vol. 15, n.º 1-2, pp. 16-25, ene. 2012.

[4] A. J. Haes, C. L. Haynes, A. D. McFarland, G. C. Schatz, R. P. Van Duyne, y S. Zou, «Plasmonic Materials for Surface-Enhanced Sensing and Spectroscopy», *MRS Bulletin*, vol. 30, n.º 5, pp. 368-375, may 2005.

[5] H. Yilmaz, S. H. Bae, S. Cao, Z. Wang, B. Raman, y S. Singamaneni, «Gold-Nanorod-Based Plasmonic Nose for Analysis of Chemical Mixtures», *ACS Applied Nano Materials*, vol. 2, n.º 6, pp. 3897-3905, jun. 2019.
[6] N. Yang, T.-T. You, Y.-K. Gao, C.-M. Zhang, y P.-G. Yin, «Fabrication of a Flexible Gold Nanorod Polymer Metafilm via a Phase Transfer Method as a SERS Substrate for Detecting Food Contaminants», *Journal of Agricultural and Food Chemistry*, vol. 66, n.º 26, pp. 6889-6896, jul. 2018.
[7] Y. Yu *et al.*, «Gold-Nanorod-Coated Capillaries for the SERS-Based Detection of Thiram», *ACS Applied Nano Materials*, vol. 2, n.º 1, pp. 598-606, ene. 2019.
[8] B. Nikoobakht y M. A. El-Sayed, «Preparation and Growth Mechanism of Gold Nanorods (NRs) Using Seed-Mediated Growth Method», *Chemistry of Materials*, vol. 15, n.º 10, pp. 1957-1962, may 2003.
[9] A. Sambou, P. D. Tall, y K. Talla, «Control of the Surface Plasmon Resonance of Two Configurations of Nanoparticles: Simple Gold Nanorod and Gold/Silica Core/Shell», *Nanoscience and Nanotechnology Research*, p. 6.
[10] P. Singh, T. A. F. König, y A. Jaiswal, «NIR-Active Plasmonic Gold Nanocapsules Synthesized Using Thermally Induced Seed Twinning for Surface-Enhanced Raman Scattering Applications», *ACS Applied Materials & Interfaces*, vol. 10, n.º 45, pp. 39380-39390, nov. 2018.
[11] X. Huang, S. Neretina, y M. A. El-Sayed, «Gold Nanorods: From Synthesis and Properties to Biological and Biomedical Applications», *Advanced Materials*, vol. 21, n.º 48, pp. 4880-4910, dic. 2009.
[12] Z. Zheng, T. Tachikawa, y T. Majima, «Single-Particle Study of Pt-Modified Au Nanorods for Plasmon-Enhanced Hydrogen Generation in Visible to Near-Infrared Region», *Journal of the American Chemical Society*, vol. 136, n.º 19, pp. 6870-6873, may 2014.
[13] J. Xavier, S. Vincent, F. Meder, y F. Vollmer, «Advances in optoplasmonic sensors – combining optical nano/microcavities and photonic crystals with plasmonic nanostructures and nanoparticles», *Nanophotonics*, vol. 7, n.º 1, pp. 1-38, ene. 2018.
[14] N. R. Jana, L. Gearheart, y C. J. Murphy, «Seed-Mediated Growth Approach for Shape-Controlled Synthesis of Spheroidal and Rod-like Gold Nanoparticles Using a Surfactant Template», *Advanced Materials*, vol. 13, n.º 18, pp. 1389-1393, sep. 2001.
[15] C. J. Orendorff y C. J. Murphy, «Quantitation of Metal Content in the Silver-Assisted Growth of Gold Nanorods», *The Journal of Physical Chemistry B*, vol. 110, n.º 9, pp. 3990-3994, mar. 2006.
[16] X. Xu *et al.*, «Effect of shell thickness on small-molecule solar cells enhanced by dual plasmonic gold-silica nanorods», *Applied Physics Letters*, vol. 105, n.º 11, p. 113306, sep. 2014.
[17] M. Shanthil, H. Fathima, y K. George Thomas, «Cost-Effective Plasmonic Platforms: Glass Capillaries Decorated with Ag@SiO_2 Nanoparticles on Inner Walls as SERS Substrates», *ACS Applied Materials & Interfaces*, vol. 9, n.º 23, pp. 19470-19477, jun. 2017.
[18] J. Chen, R. Zhang, L. Han, B. Tu, y D. Zhao, «One-pot synthesis of thermally stable gold@mesoporous silica core-shell nanospheres with catalytic activity», *Nano Research*, vol. 6, n.º 12, pp. 871-879, dic. 2013.
[19] M. N. Sanz-Ortiz, K. Sentosun, S. Bals, y L. M. Liz-Marzán, «Templated Growth of Surface Enhanced Raman Scattering-Active Branched Gold Nanoparticles within Radial Mesoporous Silica Shells», *ACS Nano*, vol. 9, n.º 10, pp. 10489-10497, oct. 2015.
[20] N. Chemin, M. Klotz, V. Rouessac, A. Ayral, y E. Barthel, «Mechanical properties of mesoporous silica thin films: Effect of the surfactant removal processes», *Thin Solid Films*, vol. 495, n.º 1-2, pp. 210-213, ene. 2006.
[21] W. Zeng, X.-F. Qian, Y.-B. Zhang, J. Yin, y Z.-K. Zhu, «Organic modified mesoporous MCM-41 through solvothermal process as drug delivery system», *Materials Research Bulletin*, vol. 40, n.º 5, pp. 766-772, may 2005.

[22] L. Scarabelli, M. Grzelczak, y L. M. Liz-Marzán, «Tuning Gold Nanorod Synthesis through Prereduction with Salicylic Acid», *Chemistry of Materials*, vol. 25, n.º 21, pp. 4232-4238, nov. 2013.
[23] I. Pastoriza-Santos, J. Pérez-Juste, y L. M. Liz-Marzán, «Silica-Coating and Hydrophobation of CTAB-Stabilized Gold Nanorods», *Chemistry of Materials*, vol. 18, n.º 10, pp. 2465-2467, may 2006.
[24] G. Büchel, R. Denoyel, P. L. Llewellyn, y J. Rouquerol, «In situ surfactant removal from MCM-type mesostructures by ozone treatment», *Journal of Materials Chemistry*, vol. 11, n.º 2, pp. 589-593, 2001.
[25] J. Pérez-Juste, L. M. Liz-Marzán, S. Carnie, D. Y. C. Chan, y P. Mulvaney, «Electric-Field-Directed Growth of Gold Nanorods in Aqueous Surfactant Solutions», *Advanced Functional Materials*, vol. 14, n.º 6, pp. 571-579, jun. 2004.

ANNEX I

Template removal calculation of AuNR@mSiO$_2$ after a reflux of 40 minutes in HCl (0.1M) in ethanol.

Table 6. Data recompilation of the TGA results for AuNR@mSiO$_2$ with template and after a reflux of 10 minutes with HCl (0.1M)

Experience	Weight (%) at 800 ºC	% CTAB removed
AuNR@mSiO$_2$ with template	59.27	0
AuNR@mSiO$_2$ after 10 min HCl(0.1 M)	86.48	77.33

We assume a calculation basis of 100 mg:

From the total weight of a sample, 86.48 mg correspond only to Au-SiO$_2$, and the rest is CTAB, 13.52 mg. For this reason, de CTAB/Au-SiO$_2$ ratio present in all the sample of the same synthesis batch is 0.687.

Next, we will calculate the amount of CTAB present in the treated sample.

$$\frac{\text{Au}-\text{SiO}_2}{\text{CTAB}} = 0.687 \rightarrow \left(\frac{\text{Au}-\text{SiO}_2}{\text{CTAB}}\right)_{\text{HCl (0.1M)}} = 0.687 = \frac{86.48}{\text{CTAB}} \rightarrow \text{CTAB} = 59.64 \text{ mg}$$

$$\%_{\text{removed}} = \frac{59.64 - 13.52}{59.64} = 77.33\ \%$$

ANNEX II

Firstly, to approximate the final thickness of the shell with a template, it is necessary to set some parameters such as the dimension of the gold nanorods (10nm x 40 nm), the geometry of the silica pores (cylindrical) and the dimension of the complete Au and SiO_2 particle (120 nm diameter).

Below we calculate the different volumes of the parts that make up the nanostructure.

$$V_{sphere\ (Au-SiO2)} = \frac{4}{3}\pi\, r^3 = \frac{4}{3}\pi\,(60\ nm)^3 = 904\,781\ nm^3$$

$$V_{AuNR} = \pi\, r^2 h = \pi\,(10\ nm)^2\ 40 = 3\,142\ nm^3$$

$$V_{SiO2-CTAB} = V_{sphere\,(Au-SiO2)} - V_{AuNR} = 904\,781 - 3\,142 = 901\,639\ nm^3$$

Next, we use the gold-silica/surfactant ratio (ANNEX I) considering this constant for all synthesized nanostructures.

$$\frac{\mathrm{Au} - \mathrm{SiO_2}}{\mathrm{CTAB}} = 0.70$$

$$\rho_{\mathrm{Au}} = 19.3\ \mathrm{g/cm^3} \rightarrow \rho_{\mathrm{Au}} = 19.3\,\frac{\mathrm{g}}{\mathrm{cm^3}}\,\frac{1\ cm^3}{((10^7)^3)\ nm^3} = 19.3\ 10^{-21}\, g/nm^3$$

$$\mathrm{m_{Au}} = \mathrm{V_{AuNR}}\ \rho_{\mathrm{AuNR}} = 6.064\ 10^{-17}\,\mathrm{g\ Au}$$

$$\rho_{\mathrm{SiO\ 2\ dense}} = 2.2\,\frac{\mathrm{g}}{\mathrm{cm^3}} \rightarrow \mathrm{m_{SiO\ 2\ dense}} = 2.2\,\frac{\mathrm{g}}{10^{21}\,\mathrm{nm^3}}\,901\,639\ nm^3$$
$$= 1.983\ 10^{-15}\, g\ SiO_2 - CTAB$$

Now, with the data obtained in the TGA of the MCM41 we obtain the ratio CTAB/SiO_2 porous (1.0837) in the same way as in Annex I, and thus calculate the amount of porous silica present.

$$\frac{\mathrm{CTAB}}{\mathrm{SiO_2\ porose}} = \frac{52.01}{47.99} = 1.084$$

$$m_{SiO\ 2\ porose} = 9.52\ 10^{-16} g$$

$$m_{CTAB} = 1.983\ 10^{-15} - 9.52\ 10^{-16} = 1.03\ 10^{-15}\ g$$

Then, you can calculate how much 1 nanoparticle of AuNR@mSiO2 weighs without surfactant.

$$m_{AuNR\ @mSiO\ 2} = 6.064\ 10^{-17} + 9.52\ 10^{-16}$$
$$= 1.012\ 10^{-15}\ g \text{ of AuNR@mSiO}_2 \text{ with the template 100 \% removed}$$

The total area of the pores is calculated as follows:

$$S_{pores} = 9.52\ 10^{-16}\ g\ SiO_2\ porose\ x\ 0.895\ cm^3 of\ pores$$
$$= 8.52\ 10^{-15} cm^3 of\ pores = 852\ 040\ nm^3\ of\ pores$$

$$V_{SiO2porose} = V_{SiO2-CTAB} - V_{pores} = 901\ 639 - 852\ 040 = 49\ 599\ nm^3$$

Table 7. Data recompilation of the volumes of each part of the nanostructure

	Volume
$V_{AuNR@mSiO2}$	904 781 nm^3
V_{AuNR}	3 142 nm^3
$V_{SiO2-CTAB}$	901 639 nm^3
$V_{SiO2\ porose}$	49 599 nm^3
Vpores	852 040 nm^3

Once the data is collected we calculate the shell thickness with template that is still present in each of the treatments (table 5). This data is calculated assuming identical pores of 3 nm diameter and 60 nm length, and considering that the elimination of the surfactant is carried out from outside to inside according to the decreasing nucleus model.

$$d_{AuNR\ @mSiO\ 2\ O3\ treatment} = 60\ nm * (1 - 0.7830) = 13.0\ nm$$

$$d_{AuNR\ @mSiO\ 2\ HCl\,(0.1M)40\ min} = 60\ nm * (1 - 0.8737) = 7.6\ nm$$

$$d_{AuNR\ @mSiO\ 2\ HCl\,(0.1M)30\ min} = 60\ nm * (1 - 0.6996) = 18.0\ nm$$

$$d_{AuNR\ @mSiO\ 2\ HCl\,(0.1M)20\ min} = 60\ nm * (1 - 0.7620) = 14.3\ nm$$

$$d_{\text{AuNR @mSiO 2 HCl (0.1M)10 min}} = 60\ \text{nm} * (1 - 0.7730) = 13.8\ \text{nm}$$